Ab initio study of the charge order and Zener polaron formation in half-doped manganites

C. de Graaf,[1,*] C. Sousa,[2] and R. Broer[3]
[1]*Department of Physical and Inorganic Chemistry, Universitat Rovira i Virgili Plaça Imperial Tàrraco 1, 43005 Tarragona, Spain*
[2]*Departament de Química Física and Parc Científic, Universitat de Barcelona C/Martí i Franquès 1, 08028 Barcelona, Spain*
[3]*Theoretical Chemistry, Materials Science Centre, Rijksuniversiteit Groningen Nijenborgh 4, 9747 AG Groningen, The Netherlands*
(Received 14 April 2004; revised manuscript received 30 June 2004; published 1 December 2004)

The character of the electronic ground state of $La_{0.5}Ca_{0.5}MnO_3$ has been addressed with quantum chemical calculations on large embedded clusters. We find a charge ordered state for the crystal structure reported by Radaelli *et al.* [Phys. Rev. B **55**, 3015 (1997)] and Zener polaron formation in the crystal structure with equivalent Mn sites proposed by Daoud-Aladine *et al.* [Phys. Rev. Lett. **89**, 097205 (2002)]. Important O to Mn charge transfer effects are observed for the Zener polaron.

DOI: 10.1103/PhysRevB.70.235104 PACS number(s): 75.47.Lx, 71.15.Ap, 71.27.+a

I. INTRODUCTION

A common classification of the manganites is based on the bandwidth of the partially occupied band formed by the Mn-3*d* orbitals of e_g-like character.[1–3] The small bandwidth manganites such as $Pr_{(1-x)}Ca_xMnO_3$ show a charge ordered (CO) phase at half doping, whereas this phase is absent in the large bandwidth systems (e.g., $La_{0.5}Sr_{0.5}MnO_3$). In the present study we will focus on the electronic ground state of $La_{1-x}Ca_xMnO_3$ at half doping. This compound has been classified as an intermediate bandwidth manganite[1] with characteristics of both small bandwidth systems (CO phases) and large bandwidth systems (a ferromagnetic metallic phase). For a long time the electronic groundstate of $La_{0.5}Ca_{0.5}MnO_3$ has been considered as a CO phase of Mn^{3+} and Mn^{4+} ions, where the magnetic moments show CE-type ordering.[4–6]

The local valence electron configuration on a Mn^{3+} ion is $3d^4$. In octahedral symmetry the weak-field ground state is ^5E_g. This state is orbitally degenerate and therefore unstable with respect to distortions: it is Jahn-Teller active.[7,8] On the other hand, the three 3*d* electrons of a Mn^{4+} ion occupy three degenerate orbitals of t_{2g} symmetry and this leads to an $^4A_{2g}$ state, i.e., to a state that is orbitally nondegenerate. Such a state is not Jahn-Teller unstable.

Recently, the CO interpretation has, however, been questioned by various authors.[9–15] García and co-workers argue that the Mn K_β-edge emission spectra of the half-doped manganites cannot be resolved as a weighted average of the spectra of the respective end-members[9] as would be the case for a CO phase with Mn^{3+} and Mn^{4+}. The crystal structure determination of Daoud-Aladine and co-workers[11] for the closely related $Pr_{0.6}Ca_{0.4}MnO_3$ reveals that all Mn ions in this crystal are virtually identical. They propose an electronic ground state of so-called Zener polarons in which one e_g electron is shared by two Mn ions. Zheng and Patterson performed periodic unrestricted Hartree-Fock (UHF) calculations with the crystal structure proposed by Radaelli *et al.*[6] and find an electronic ground state formed by ferromagnetically coupled Mn^{3+}-O^--Mn^{3+} units.[12] Similar periodic UHF calculations of Ferrari, Towler, and Littlewood[13] also indicate important charge transfer (CT) effects. However, in the solution found by these authors a zig-zag ordering appears of Mn^{3+}-O^--Mn^{3+}-O^--Mn^{3+} trimers. These solutions with equivalent Mn valencies are in contrast to what can be expected from the crystal structure as proposed by Radaelli,[6] in which Jahn-Teller distorted sites alternate with nondistorted sites. In the model Hamiltonian study of Efremov, van den Brink, and Khomskii[14] different phases are observed around half doping. In addition to the Zener polaron phase and the conventional CE state, a third state was found that can be described as a superposition of the previous two.

The embedded cluster model approach offers an alternative strategy to obtain information that complements periodic UHF calculations, which are strictly monoconfigurational and do not include electron correlation effects, and model Hamiltonian studies, for which the parameter choice can be delicate. *Ab initio* cluster model calculations have been applied successfully over the last decade to derive electronic structure parameters in many oxides (see Refs. 16–18, and references therein). Recently, the methodology has been applied to study the character of the ground state in α'-NaV_2O_5.[19–21] The main conclusion of these studies is that the ground-state electron distribution of a V-O-V rung is best described by a multiconfigurational wave function with a V-$3d^1$-O-$2p^5$-V-$3d^1$ leading configuration. Here, we consider different embedded cluster models to study the electronic ground state of $La_{0.5}Ca_{0.5}MnO_3$. The proposal of Zheng and Patterson is tested with clusters with two or four Mn ions, using the crystal structure of Radaelli *et al.* as input. Similar clusters are considered to test the Zener polaron hypothesis, although we apply the crystal structure of Daoud-Aladine *et al.* in that case. Finally, the three center polaron solution of Ferrari, Towler, and Littlewood is studied with a linear cluster that contains three Mn ions.

II. CLUSTER CALCULATIONS

All clusters are completed by adding the oxygens that coordinate the Mn ions, i.e., 11 for the two-center clusters, 16 for the three-center clusters, and 21 for the L-shaped four-center clusters. The first embedding shell around the cluster contains total ion potentials (TIP's) for the Mn, La, and Ca

TABLE I. Formal charges used to generate the four different Madelung fields that embed the clusters.

Label	Description	Mn	O	La/Ca
1	Ionic, CO	3+/4+	2−	2.5+
2	Ionic, no-CO	3.5+	2−	2.5+
3	Complete CT	3+	2−/1−	2.5+
4	Partial CT	3+/3.5+	2−/1.5−	2.5+

cations coordinating the oxygens in the cluster. Around this collection of all-electron centers and TIP's, we place an array of optimized point charges that accurately reproduce the Madelung potential in the whole cluster region. The local cluster symmetry is assumed to be C_1 in all cases, i.e., no symmetry restrictions are imposed on the Hamiltonian.

Our analysis of the electronic structure is based on the complete active space self-consistent field (CASSCF) method as implemented in the MOLCAS5.4 code.[22] The CASSCF approach is sufficient for an accurate description of the electron distribution. In a recent review on molecular orbital theory, Roos and Ryde demonstrate that the CASSCF natural orbitals are very close to Full CI natural orbitals, provided the active space has been properly chosen so that all important nondynamical orvalence electron correlation is accounted for.[23] This is in contrast with studies of accurate relative energies, where the inclusion of dynamical electron correlation effects is required. Since in the present study we are concerned with determining electron distributions rather than energy differences, a CASSCF approach is adequate.

The occupied cluster orbitals are divided in inactive orbitals, which remain doubly occupied, and active orbitals, for which the occupation is optimized and can vary between 0 and 2. The orbitals in the active space are chosen in such a way that none of the plausible electronic states is favored above the others. For this purpose, we consider as active orbitals all Mn-3*d* orbitals of t_{2g}-like character, one e_g-like orbital per Mn center, and one O-2*p* orbital per bridging oxygen. No assumption is made about the spatial shape of these orbitals but they are variationally optimized with respect to the cluster energy. In this way, the orbitals can represent any type of symmetric or asymmetric orbital ordering. Adding a second Mn e_g-like orbital to the active space does not change the *N*-electron wave function. This orbital has a natural occupation number very close to zero and would only slow down the convergence of the SCF procedure due to redundant orbital rotations between this second e_g-like orbital and the nonoccupied orbitals in the virtual space. The number of active electrons is 9, 14, and 20 for the two-center, three-center, and four-center clusters, respectively. The spin multiplicity of the ground state wave function in these clusters is 8, 11, and 15. A full configuration interaction is performed within this active space.

All cluster orbitals, i.e., the inactive doubly occupied orbitals plus the active orbitals, are linear combination of a large number of basis functions centered on the different cluster atoms. For example the e_g-like active orbital is linear combination with main contribution from the 3*d*-type spherical harmonic basis functions centered on the Mn sites. Depending on the relative size of the optimized coefficients of these spherical harmonics this e_g-like orbital can be of the $3r^2-x^2$ type or $3r^2-y^2$ type or have any other spatial orientation. In short, the computational scheme chosen ensures a balanced treatment of CO configurations, ligand to metal CT effects, the delocalization of the e_g electron over two Mn centers, and the different orbital orderings.

We analyze our wave functions by their spin densities. With the extended, mutually overlapping atomic basis sets used in the present calculations, total charge analyses do not give meaningful results. Completely different electronic configurations may lead to almost the same total charges. In contrast, analysis of the spin densities gives information about the distribution of the unpaired electrons, and therewith on the delocalization of the singly occupied Mn-3*d* e_g-like orbitals.

III. Ca/La STACKING

Two computational questions have to be addressed before discussing the results. These concern the details of the crystalline environment of the clusters. In the first place, a choice must be made for the formal charges to generate a Madelung potential. In order to avoid a bias towards the CO state, we opted to embed the clusters in four different Madelung potentials. Two of them correspond to fully ionic Madelung fields and in the other two CT effects are incorporated as suggested in Refs. 12 and 13. Details are given in Table I.

The second question concerns the stacking of the La^{3+} and Ca^{2+} ions in the crystal structure. In the cluster calculations this arrangement must be made explicit to construct the first embedding shell. Since there is no direct experimental information about this stacking, we compare different choices. In the first place, a zig-zag stacking of the La and Ca ions along the interatomic Mn-Mn axis is considered. We assign either an average charge of 2.5+ (option *A*) or formal ionic charges of 3+ and 2+ (option *B*). Secondly, La^{3+} ions are placed on one side of the cluster and Ca^{2+} on the other (option *C*). For the three-center cluster, this option corresponds to putting La ions on the extremes of the cluster and Ca ions around the central Mn. The same embedding, but now with average charges is labeled with option *D*. Finally, the cluster is embedded with Ca^{2+} ions above the cluster and La^{3+} ions below it (option *E*). A detailed analysis of the fine structure of the x-ray absorption spectra in $La_{1-x}Sr_xMnO_3$, showed that there exist a certain tendency towards Sr clustering at low *x*.[24] This effect seems, however, to disappear when *x* approaches 0.5. In that case, a random distribution of La and Sr seems more adequate, which makes option *A* the most realistic one.

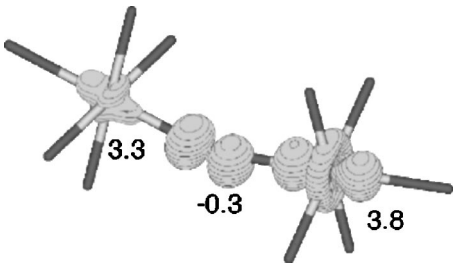

FIG. 1. Spin density maps for the two-center cluster in the Radaelli structure. The numbers give the total spin populations on the atomic centers.

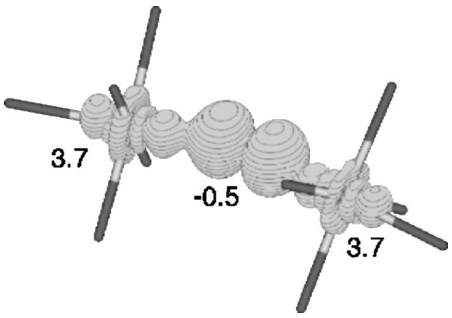

FIG. 2. Spin density maps for the two-center cluster with the structure of Daoud-Aladine *et al.* The numbers give the total spin populations on the atomic centers.

IV. RESULTS

A. Two-center clusters

Having settled the computational strategies, we now discuss the outcomes of the CASSCF calculations. The two-center cluster based on the Radaelli structure has one Jahn-Teller distorted Mn site, while the other is quasioctahedral. Hence, the electronic cluster wave function would reflect a Mn-$3d^3$–O-$2p^6$–Mn-$3d^4$ situation if the conventional CO state were the most stable one. On the other hand, a wave function characterized by a Mn-$3d^4$–O-$2p^5$–Mn-$3d^4$ configuration would confirm the ferromagnetic polaron hypothesis of Zhang and Patterson.

In all embeddings that can be obtained by combining the options mentioned previously, the leading configuration of the cluster wave function is best described as a CO state. Small CT effects are observed from the bridging oxygen to the quasioctahedral Mn site. Figure 1 shows the spin density map due to the O-$2p$ and Mn-$3d(e_g)$ electrons obtained with embedding 2*A*. This solution corresponds to the situation with the largest contribution of CT configurations. The Mn-$3d(t_{2g})$ spin density is highly localized on Mn and almost identical for both Mn ions, and is omitted for clarity. The remaining spin density illustrates the CO character of the cluster wave function. It is largely concentrated on the Jahn-Teller distorted Mn site and directed along the long Mn-O bonds. The total spin populations shown in the figure are only weakly dependent on the details of the embedding, except for option *C* (see below). The variation on the Jahn-Teller distorted site is less than 0.05 $e-$, on the bridging oxygen it ranges between −0.14 and −0.33 and for the second Mn ion between 3.08 and 3.34. The first electronic state with a complete CT from the bridging O to the Mn^{4+} site lies 1.8 eV higher in energy than the CO state. This CT state is obtained by imposing a high-spin coupling of all active electrons. Some uncertainty is contained in this relative energy because high spin coupling is assumed between the Mn and O spins. Nevertheless, the Mn-O spin coupling is only a fraction of the energy difference between the CO and CT states.

The results obtained with option *C* are of a complete different nature. Spin density appears on a nonbridging oxygen on the Ca^{2+} edge of the cluster. Apparently, the arrangement of 3+ charges on one edge of the cluster and 2+ charges on the other induces an unrealistic Coulomb potential in the cluster. The results for this stacking in the two-center clusters are not further discussed.

The Mn sites in the two-center cluster with the structure of Daoud-Aladine *et al.* have an almost equivalent local geometry. The Zener polaron formation would correspond to an electronic ground state characterized by a Mn-$3d^{3.5}$–O-$2p^6$–Mn-$3d^{3.5}$ distribution of the electrons. In most cases, the CASSCF wave functions indeed reflect two Mn ions with an equivalent number of *d* electrons, but we also find a rather strong contribution from CT configurations which was not foreseen in the original proposal of the electronic structure of the polaron.[11] The comparison of the spin density in Figs. 1 and 2 clearly illustrates the different nature of the cluster wave function in both cases. The spin density obtained with the structure of Daoud-Aladine *et al.* (Fig. 2) is delocalized over the whole cluster and equivalent Mn sites emerge. The Mn e_g-like orbitals are symmetrically ordered and of $3x^2-r^2$ character, with *x* being the interatomic Mn-Mn axis. Furthermore, we observe a significant spin density on the bridging oxygen originated from the large CT contributions to the wave function. These results are almost independent of the embedding scheme. Only with the ionic CO Madelung potential (option 1 in Table I), we obtain a CO state. However, the delocalized state with equivalent Mn sites obtained from a high spin coupling of the active electrons is significantly closer in energy in the present case ($\approx$1.3 eV) than in the previous discussed two-center cluster based on the Radaelli structure (1.8 eV).

B. Three-center cluster

The central Mn ion in the cluster that we use to test the three-center polaron solution has a Jahn-Teller distorted coordination, whereas the two Mn ions on the edge have an almost octahedral coordination. Hence, with a similar reasoning as for the two-center polaron hypothesis, the electronic wave function of the three-center clusters can reflect a CO type of state (Mn-$3d^3$–O-$2p^6$–Mn-$3d^4$–O-$2p^6$–Mn-$3d^3$), or a three-center polaron as proposed by Ferrari, Towler, and Littlewood (Mn-$3d^4$–O-$2p^5$–Mn-$3d^4$–O-$2p^5$–Mn-$3d^4$). For most of the embeddings, the character of the cluster wave function indicates a conventional CO state. Important CT effects are only found for option 1*C*, 2*C* and 4*C* and lead to an electronic charge distribution in agreement with the findings of Ferrari, Towler, and Littlewood.

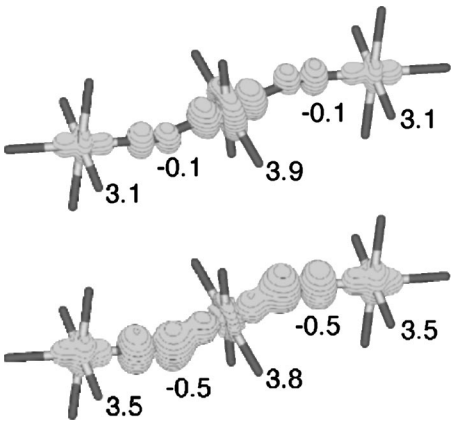

FIG. 3. Spin density maps for the three-center cluster with embedding 1*A* (upper part) and 1*C* (lower part). The numbers give the total spin populations on the atomic centers.

These findings are illustrated in Fig. 3, which compares the spin densities obtained with options 1*A* and 1*C*. For option 1*A*, we observe that the spin density due to the Mn-e_g and O-2*p* electrons is almost completely concentrated on the central Mn, revealing the ionic CO character of the cluster wave function. The total spin populations also reflect the CO character for this option with only minor CT effects. This picture changes dramatically for option 1*C*. We now see a more delocalized spin density with almost equal contributions from the three Mn ions and a significant spin density on the bridging oxygens. The ordering of the Mn-3d(e_g) orbitals is identical to that found by Ferrari, Towler, and Littlewood. The negative spin populations on the bridging oxygens of −0.5 indicate important CT effects with a low-spin coupling between the O-2*p* electron and the Mn-3*d* electrons. However, this particular stacking of La^{3+} and Ca^{2+} cannot be realized in a periodic structure. Hence, we conclude that the most probable electronic structure in the three-center cluster corresponds to a conventional CO type state with rather small CT effects. The energy of the state with bridging O^- ions and Mn^{3+} is ≈3.8 eV above the CO state in the more realistic embeddings. These findings also indicates that the three-center polaron solution is highly improbable.

The Madelung potential obtained by assuming a complete CT between O and Mn (options 3 *A*-*E*) leads to the appearance of spin density on nonbridging oxygens. This effect is due to the ordering of the O^- stripes in the crystal proposed by Ferarri, Towler, and Littlewood. Perpendicular to the stripe direction, each row of O ions sees an O^- stripe on one side and a normal array of O^{2-} charges on the other. When this is reflected in the Madelung field that embeds the cluster, the hole localizes in the neighborhood of the −2 charges.

C. Four-center cluster

The stability of the results discussed above against the cluster size effects is checked with the L-shaped four-center clusters. The wave function can reflect a CO state, the Zener polaron solution (two separated polarons) or alternatively the e_g electrons can be delocalized over all four Mn sites. The results are in full agreement with those obtained in the two-center clusters. For the Radaelli structure, we obtain a CO state with small CT effects. Applying the Daoud-Aladine structure, our CASSCF calculations show two identical polarons (see Fig. 4) separated by an oxygen with no spin density. The active space does include CT configurations from the oxygen that bridges the two polarons but their contribution to the *N*-electron wave function is found to be negligible. This means that the Mn-e_g electrons are localized within the two-center polaron and that CT effects only take place within each polaron.

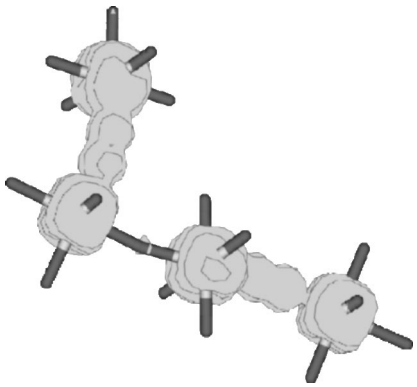

FIG. 4. Total spin density maps for the *L*-shaped four-center cluster with the Daoud-Aladine structure.

V. CONCLUSIONS

In summary, the cluster calculations indicate that the structure proposed by Radaelli *et al.* with Jahn-Teller and quasioctahedral sites leads to a CO state. The Jahn-Teller site pins a Mn^{3+} ion, leaving a Mn^{4+} on the nondistorted site. These findings are in agreement with the results of the periodic density functional theory calculations reported by Popović and Satpathy,[25] who also argue that the Jahn-Teller distortion is the leading mechanism for CO. We find a small but significant CT from O^{2-} to the Mn^{4+} site. The nondistorted Mn coordination in the Daoud-Aladine structure leads to a delocalization of the e_g electron over the two Mn sites, i.e., to Zener polaron formation. We modify the original idea by proposing an important CT effect from O to both Mn sites. The four-center clusters confirm these results. We recognize two separate polarons for the Daoud-Aladine structure.

ACKNOWLEDGMENTS

Financial support has been provided by Netherlands National Computer Facilities Foundation (NCF), the Spanish Ministry of Science and Technology (Project No. BQU2002-04029-C02-01/02), and the Generalitat de Catalunya (Grants Nos. 2003BEAI400286 and ACI2002-15).

*Electronic address: coen@quimica.urv.es

[1] E. Dagotto, T. Hotta, and A. Moreo, Phys. Rep. **344**, 1 (2001).
[2] J. B. Goodenough and J.-S. Zhou, *Localized to Itinerant Electronic Transition in Perovskite Oxides* (Springer Verlag, Berlin, New York, 2001), pp. 17–113.
[3] M. B. Salamon and M. Jaime, Rev. Mod. Phys. **73**, 583 (2001).
[4] E. O. Wollan and W. C. Koehler, Phys. Rev. **100**, 545 (1955).
[5] C. H. Chen and S.-W. Cheong, Phys. Rev. Lett. **76**, 4042 (1996).
[6] P. G. Radaelli, D. Ē Cox, M. Marezio, and S.-W. Cheong, Phys. Rev. B **55**, 3015 (1997).
[7] J. S. Griffith, *The Theory of Transition Metal Ions* (Cambridge University Press, Cambridge, 1971), pp. 209–211.
[8] P. A. Cox, *Transition Metal Oxides* (Clarendon Press, Oxford, 1995), pp. 40–42.
[9] J. García, M. C. Sánchez, J. Blasco, G. Subías, and M. G. Proietti, J. Phys.: Condens. Matter **13**, 3243 (2001).
[10] J. Rodríguez-Carvajal, A. Daoud-Aladine, L. Pinsard-Gaudart, M. T. Fernandez-Díaz, and A. Revcolevschi, Physica B **320**, 1 (2002).
[11] A. Daoud-Aladine, J. Rodríguez-Carvajal, L. Pinsard-Gaudart, M. T. Fernandez-Díaz, and A. Revcolevschi, Phys. Rev. Lett. **89**, 097205 (2002).
[12] G. Zheng and C. H. Patterson, Phys. Rev. B **67**, 220404 (2003).
[13] V. Ferrari, M. D. Towler, and P. B. Littlewood, Phys. Rev. Lett. **91**, 227202 (2003).
[14] D. V. Efremov, J. van den Brink, and D. I. Khomskii, cond-mat/0306651 (unpublished).
[15] K. J. Thomas *et al.*, Phys. Rev. Lett. **92**, 237204 (2004).
[16] A. Klimkans and S. Larsson, J. Chem. Phys. **115**, 466 (2001).
[17] I. de P. R. Moreira, N. Suaud, N. Guihery, J. P. Malrieu, R. Caballol, J. M. Bofill, and F. Illas, Phys. Rev. B **66**, 134430 (2002).
[18] C. J. Calzado, C. de Graaf, E. Bordas, R. Caballol, and J.-P. Malrieu, Phys. Rev. B **67**, 132409 (2003).
[19] N. Suaud and M.-B. Lepetit, Phys. Rev. Lett. **88**, 056405 (2002).
[20] L. Hozoi, A. H. de Vries, A. B. van Oosten, R. Broer, J. Cabrero, and C. de Graaf, Phys. Rev. Lett. **89**, 076407 (2002).
[21] L. Hozoi, C. Presura, C. de Graaf, and R. Broer, Phys. Rev. B **67**, 035117 (2003).
[22] K. Andersson *et al.*, *Molcas version 5.4*, Department of Theoretical Chemistry, University of Lund, 2002.
[23] B. O. Roos and U. Ryde, in *Comprehensive Coordination Chemistry 2*, edited by B. Lever (Elsevier, Amsterdam, the Netherlands, 2003), Vol. 1.
[24] T. Shibata, B. Bunker, J. F. Mitchell, and P. Schiffer, Phys. Rev. Lett. **88**, 207205 (2002).
[25] Z. Popović and S. Satpathy, Phys. Rev. Lett. **88**, 197201 (2002).